Physical Chemistry

Isomerism in $OBe_3F_3^+$ cation: an *ab initio* study

N. M. Klimenko,[a] E. A. Rykova,[a] M. L. McKee,[b] and I. N. Senchenya[c]*

[a]*M. V. Lomonosov Moscow State Academy of Fine Chemical Technology, 86 prosp. Vernadskogo, 117571 Moscow, Russian Federation. Fax: +7 (095) 430 7983. E-mail: klimenko@mitht.msk.su*

[b]*Department of Chemistry, Auburn University, Auburn, Alabama 36849-5312, USA. Fax: +1 (334) 844 6959. E-mail: mckee@chem.auburn.edu*

[c]*N. D. Zelinsky Institute of Organic Chemistry, Russian Academy of Sciences, 47 Leninsky prosp., 117913 Moscow, Russian Federation. Fax: +7 (095) 135 5328. E-mail: is@ioc.ac.ru*

Ab initio MP2/6-31G*//HF/6-31G*+ZPE(HF/6-31G*) calculations of the potential energy surface in the vicinity of stationary points and the pathways of intramolecular rearrangements between low-lying structures of the $OBe_3F_3^+$ cation detected in the mass spectra of μ_4-$Be_4O(CF_3COO)_6$ were carried out. Ten stable isomers with di- and tricoordinate oxygen atoms were localized. The relative energies of six structures lie in the range 0—8 kcal mol^{-1} and those of the remaining four structures lie in the range 20—40 kcal mol^{-1}. Two most favorable isomers, a C_{2v} isomer with a dicoordinate oxygen atom, planar six-membered cycle, and one terminal fluorine atom and a pyramidal C_{3v} isomer with a tricoordinate oxygen atom and three bridging fluorine atoms, are almost degenerate in energy. The barriers to rearrangements with the breaking of one fluorine bridge are no higher than 4 kcal mol^{-1}, except for the pyramidal C_{3v} isomer (~16 kcal mol^{-1}). On the contrary, rearrangements with the breaking of the O—Be bond occur with overcoming of a high energy barrier (~24 kcal mol^{-1}). A planar D_{3h} isomer with a tricoordinate oxygen atom and linear O—Be—H fragments was found to be the most favorable for the $OBe_3H_3^+$ cation, a hydride analog of the $OBe_3F_3^+$ ion; the energies of the remaining five isomers are more than 25 kcal mol^{-1} higher.

Key words: $OBe_3F_3^+$ and $OBe_3H_3^+$ cations, potential energy surface, structure, stability, isomerism, intramolecular rearrangements, transition states, potential energy barriers, *ab initio* calculations.

An intense peak corresponding to an $OBe_3F_3^+$ cation of unknown structure was observed in a mass spectrometric study[1] of μ_4-$Be_4O(CF_3COO)_6$ vapors. It has been suggested[1] that the $OBe_3F_3^+$ cation has a planar structure of a regular triangle with a tricoordinate O atom at its center and linear O—Be—F fragments (D_{3h}). At first glance, such a suggestion seems to be justified by analogy with the structures of onium cations of alkali metals, OL_3^+ (OK_3^+, OCs_3^+, *etc.*[2]). According to *ab initio* calculations,[3—6] the OLi_3^+ cation has a planar trigonal

Translated from *Izvestiya Akademii Nauk. Seriya Khimicheskaya*, No. 3, pp. 420—430, March, 1999.

1066-5285/99/4803-0417 $22.00

structure (D_{3h}). In principle, the $OM_3X_3^+$ cations, where M is an alkaline-earth metal and X is a univalent substituent (X = H, Hal), can be built from OL_3^+ cations by replacement of the alkali metal L by an isolobal MX group. Indeed, the calculations[7,8] have shown that the global minimum on the potential energy surface (PES) corresponds to the most favorable isomer of the $OBe_3H_3^+$ cation (a hydride analog of the $OBe_3F_3^+$ cation) with D_{3h} symmetry. At the same time, a direct analogy between onium cations of alkali metals and $OM_3X_3^+$ ions may be oversimplified, because new isomers of the latter ions can exist due to the ability of X substituents to form three-center bridging M—X_b—M′ bonds (hereafter bridging X atoms are denoted by subscript "b"). The presence of three bridging bonds leads to a pyramidal (or quasi-pyramidal) C_{3v} structure with adjacent four-membered OM_2X cycles. Intermediate forms with one and two M—X_b—M′ bridges can also be formed. According to calculations,[7,8] the energy of the pyramidal C_{3v} structure of the $OBe_3H_3^+$ cation corresponding to a local minimum on the PES is about 25 kcal mol^{-1} higher than that of the most favorable D_{3h} isomer* with three terminal H_t atoms (hereafter terminal X atoms are denoted by subscript "t").

It has been mentioned[8] that the relative stability of the structures is determined by several factors including the number of O—Be bonds, *i.e.*, by the coordination number (*CN*) of oxygen atom (*CN*(O)), the relative stability of three-center bridging M—X_b—M′ bonds compared to that of two-center M—X_t bonds, the electrostatic repulsion between the metal atom and the O and X atoms in the four-membered OM_2X cycles, by strain in the cycles, by the contribution of donor-acceptor O→M and X→M π-bonds in planar structures, *etc.* The relative stability of the structures can substantially vary upon replacement of M or X atoms by their analogs in the subgroups of the Periodic system. Since the Be—F_b—Be′ fluoride bridges are stronger than the hydride Be—H_b—Be′ bridges and the F→Be π-bonds can be formed in planar structures, it should be expected that the relative arrangement of the structures of the fluoride $OBe_3F_3^+$ cation and its hydride analog, the $OBe_3H_3^+$ cation, on the energy scale will differ and that their most favorable structures can also be different.

The aim of this study was: (1) to find the structures and to determine their relative stabilities, frequencies, and intensities of normal vibrations of the most favorable isomer of the $OBe_3F_3^+$ cation, its hydride analog, the $OBe_3H_3^+$ cation, and their low-lying isomers; (2) to localize the transition states and to evaluate the potential energy barriers to intramolecular rearrangements between the isomers; and (3) to reveal differences and similarity in the structure—energy diagrams of the $OBe_3F_3^+$ and $OBe_3H_3^+$ cations.

* The planar three-bridge D_{3h} structure has one imaginary frequency, is energetically unstable, and decomposes with elimination of BeH_2 or BeH^+.

Calculation procedure

The initial set of configurations (**1**—**10**, Fig. 1) of $OBe_3X_3^+$ (X = H, F) cations whose geometric parameters should be optimized included the above-mentioned structures **1** and **4** with C_{3v} and D_{3h} symmetry, respectively, and the structures **2**, **3**, and **7**—**9**, which can be built from the three types, **A**—**C**, of isomers of OBe_3X_4 (X = H, F) molecules[7—9] corresponding to low-lying energy minima on the PES by eliminating an X^- anion from different positions. For instance, the forms **3**, **4**, and **9** can be built from structure **A**; the configurations **2** and **3** can be built from structure **B**; and the structures **7** and **8** can be built from structure **C** (see Fig. 1). Moreover, according to calculations,[7—9] there are two additional types, **D** and **E**, of isomers characteristic of OBe_4X_6 (X = H, F) molecules, which also correspond to low-lying energy minima on the PES. The former contains a planar six-membered cycle and the latter contains a chain of two four-membered cycles lying in mutually perpendicular planes.

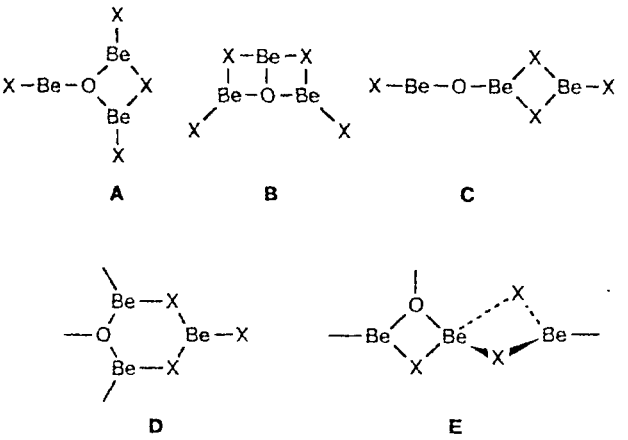

Therefore, our study of $OBe_3X_3^+$ cations also included the structures **6** and **10** related respectively to the forms **D** and **E**. Since the structure **6** can be considered as a bidentately coordinated ion pair formed by the OBe_2^{2+} dication and a BeX_3^- anion, we also optimized its tridentately coordinated form **5**. Consideration of several additional low-symmetric structures showed that all of them either are barrierlessly transformed into isomers **1**—**10** or appear to be energetically unfavorable upon geometry optimization; for this reason, they are not discussed in this study.

Among the ten structures selected, the isomers **1**—**4** and **9** contain a tricoordinate O atom, while the remaining forms contain a dicoordinate O atom. The forms **1**—**4**, which can be described by the general formula $OBe_3(X_b)_k(X_t)_{3-k}^+$ ($0 < k < 3$), differ from one another in the number of terminal X_t and bridging X_b atoms. In these structures the O atom is included in the four-membered OBe_2X cycle or the angular (or linear) O—Be—X fragment, and the *CN* of the Be atom (*CN*(Be)) is equal to 2 or 3, respectively. In structure **9** containing the OBe_2X cycle one of the Be atoms with *CN*(Be) = 1 is a terminal atom bonded to the O atom only. The forms with *CN*(O) = 2 are more varied, since the O atom can be a constituent of linear Be—O—Be′ groups (structures **7** and **8**), four-membered cycles (form **10**), or six-membered cycles (configurations **5** and **6**). In these structures, also containing four-membered XBe_2X cycles, the *CN*(Be) varies from 1 (structure **8**) to 4 (structure **10**). Most

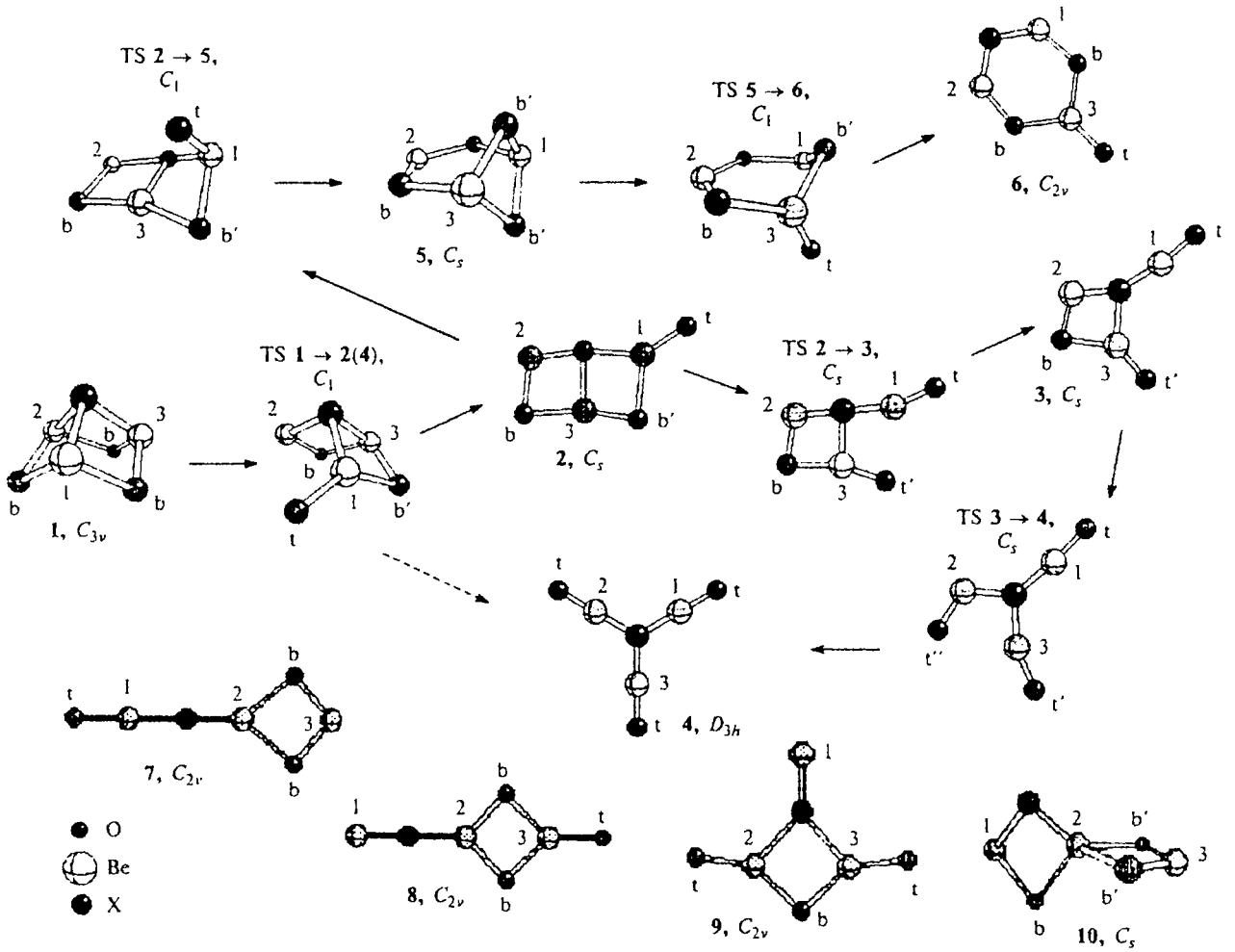

Fig. 1. Structures of isomers **1**—**10** and transition states (TS) of intramolecular rearrangements of $OBe_3X_3^+$ (X = H, F) ions; b and t are bridging (X_b) and terminal (X_t) atoms; geometrically equivalent atoms are shown by equal number of primes.

of the configurations are planar (except for structures **1**, **5**, and **10**). All three OBe_2X cycles in structure **1** and the XBe_2X cycles in structures **5** and **10** are nonplanar.

According to preliminary calculations by the Hartree—Fock method using the 3-21G basis set (HF/3-21G), the relative energies of isomers **1**—**6** of the fluoride $OBe_3F_3^+$ ion lie in the range 0—10 kcal mol^{-1}, while those of the remaining isomers are significantly higher (30—60 kcal mol^{-1}). The most favorable structure **4** (X = H) of the hydride $OBe_3H_3^+$ ion lies on the energy scale more than 50 kcal mol^{-1} lower than the other forms. To elucidate whether the structures **1**—**6** (X = F) correspond to kinetically stable isomers of the $OBe_3F_3^+$ ion, in the framework of the HF/3-21G approximation the PES was scanned along the minimum energy pathways of intramolecular rearrangements between these structures, occurring with the breaking of both fluoride bridges and the O—Be bond, and corresponding transition states were localized. As was expected, the rearrangements with the simultaneous breaking of several fluoride bridges are strongly hampered. On the contrary, the barriers to rearrangements **1** → **2** (C_1), **2** → **3** (C_s), **3** → **4** (C_s), and **5** → **6** (C_1) with the breaking of one fluoride bridge at each stage are substantially lower, though remaining appreciable (6—9 kcal mol^{-1}, except for the rearrangement **1** → **2** with the barrier of ~20 kcal mol^{-1}). The energy barriers to rearrangements **2** → **5** (C_1) and **3** → **6** (C_1) with the breaking of the O—Be bond and simultaneous formation of one fluoride bridge are rather high (~25 kcal mol^{-1}).

At the second stage we performed more accurate calculations of the PES in the vicinity of the minima and saddle points (thereafter singular points) corresponding to the structures **1**—**10** and to the transition states of rearrangements between the isomers **1**—**6** of $OBe_3X_3^+$ (X = H, F) cations. Optimization of geometric parameters and calculations of the frequencies of normal vibrations and zero-point vibrational energies (*ZPE*) were carried out in the HF/6-31G* (thereafter HF) approximation. The relative energies at the singular points were refined with inclusion of electron correlation at the second-order Møller—Plesset level of perturbation theory (in the MP2/6-31G*//HF/6-31G* approximation for X = F and in the MP2/6-31G**//HF/6-31G* approximation for X = H; thereafter MP2) both without ($E_{rel,1}$) and with ($E_{rel,2}$) inclusion of *ZPE* corrections. The same procedure was used in

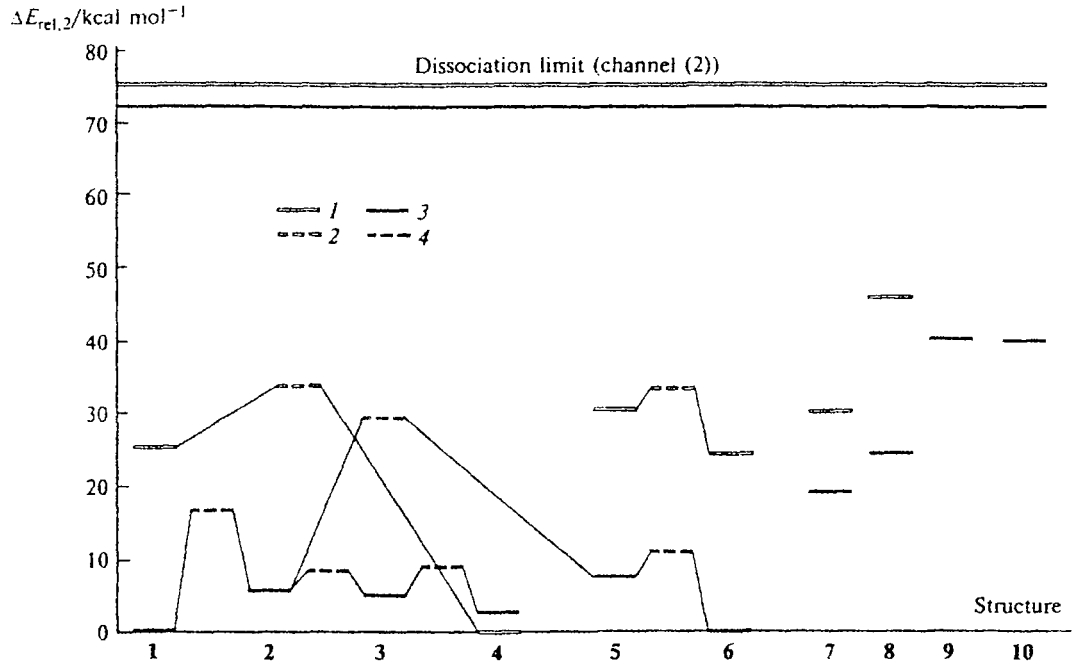

Fig. 2. Structure-energy diagram of isomers and transition states (TS) of intramolecular rearrangements of $OBe_3X_3^+$ cations, where X = H (*1*, *2*), F (*3*, *4*): *1*, $OBe_3H_3^+$ cation; *2*, TS for $OBe_3H_3^+$; *3*, $OBe_3F_3^+$ cation; and *4*, TS for $OBe_3F_3^+$.

calculations[10] of the products of monomolecular decomposition through the channels

$$OBe_3X_3^+ \rightarrow OBe_2X_2 + BeX^+, \quad (1)$$

$$OBe_3X_3^+ \rightarrow OBe_2X^+ + BeX_2. \quad (2)$$

The HF and MP2 calculations were carried out using the GAMESS-94 [11] and GAUSSIAN-94 [12] programs on SGI and SUN workstations at Auburn University (Auburn, Alabama, USA) and on a Power Challenger workstation at the N. D. Zelinsky Institute of Organic Chemistry, Russian Academy of Sciences. The results obtained are shown in Figs. 1, 2 and listed in Tables 1—6. Selected data for $OBe_3X_3^+$ cations were reported earlier.[13,14]

Results and Discussion

From the data in Tables 1 and 2 it follows that within the framework of the HF approximation all ten structures of the $OBe_3F_3^+$ cation have only real frequencies and correspond to local minima on the PES. In the MP2 approximation the $E_{rel,2}$ values of the six low-lying isomers (**1**—**6**, X = F) lie in the range from 0 to 8 kcal mol^{-1}, those of the next two isomers (**7** and **8**, X = F) lie in the range from 19 to 25 kcal mol^{-1}, and the $E_{rel,2}$ values of the two high-lying isomers (**9** and **10**, X = F) lie in the interval from 40.0 to 40.5 kcal mol^{-1}. All isomers are stable to decomposition; the dissociation limit calculated for the most favorable isomer **6** of the $OBe_3F_3^+$ cation is equal to 87 and 72 kcal mol^{-1} for channels (1) and (2), respectively.

The calculations did not support the assumption[1] that the most favorable structure of the $OBe_3F_3^+$ cation is planar structure **4*** of D_{3h} symmetry; isomers **1** and **6**, which are almost degenerate in energy, appeared to be the most stable. The isomers **2** and **3** (X = F) also have very close energies (the difference in the $E_{rel,2}$ values is ~0.2 kcal mol^{-1}); the structures **4** and **5** (X = F) are less stable than the structure **6** ($\Delta E_{rel,2} \approx 3$ and 8 kcal mol^{-1}, respectively). The energies of isomers **7** and **8** obtained from the structure **C** of the OBe_3F_4 molecule differ by about 5 kcal mol^{-1}. Finally, the difference between the $E_{rel,2}$ values for isomers **9** and **10** (X = F) does not exceed 0.3 kcal mol^{-1}.

The structure—energy diagram of the $OBe_3H_3^+$ hydride ion is quite different (see Fig. 2). Six isomers, **1** and **4**—**8**, of this cation were localized within the framework of the HF approximation, while the other four isomers are barrierlessly transformed into the former (see note to Table 1). A global minimum on the PES corresponds to isomer **4** (X = H) of D_{3h} symmetry. The isomers **1** and **6** (X = H) with the closest-lying $E_{rel,2}$ energies are ~25 kcal mol^{-1} less stable than the structure **4**. The differences in the $E_{rel,2}$ values for structures

* Our MP2 calculations showed that the energy of the pyramidal isomer **1** (X = F) is merely 0.6 kcal mol^{-1} higher than that of the planar isomer **6** (X = F). According to calculations in the MP2(full) approximation, the isomer **1** appears to be 0.1 kcal mol^{-1} more stable than isomer **6** (see note to Table 1).

Table 1. Total (E_{tot}/au), relative ($E_{rel,1}$ and $E_{rel,2}$/kcal mol^{-1})[a] energies, and zero-point vibrational energies (*ZPE*/kcal mol^{-1}) of isomers, transition states (TS) of intramolecular rearrangements, and decomposition products[b] of $OBe_3X_3^+$ (X = H, F) cations calculated at different levels of theory

Structure, TS (channel)	Symmetry	*CN*(O)	Number X_b	HF				MP2[c]		
				E_{tot}	*ZPE*	$E_{rel,1}$	$E_{rel,2}$	E_{tot}	$E_{rel,1}$	$E_{rel,2}$
				$OBe_3F_3^+$ cation						
1	C_{3v}	3	3	−417.24419	14.8	5.6	6.6	−418.05150	−0.3	0.6
2	C_s	3	2	−417.23894	13.8	8.8	8.8	−418.04184	5.8	5.8
3	C_s	3	1	−417.24244	13.3	6.7	6.2	−418.04126	6.1	5.6
4	D_{3h}	3	0	−417.24431	12.7	5.5	4.4	−418.04426	4.2	3.1
5	C_s	2	3	−417.23526	14.3	11.2	11.7	−418.03922	7.4	7.9
6	C_{2v}	2	2	−417.25318	13.8	0	0	−418.05097	0	0
7	C_{2v}	2	2	−417.22143	13.1	19.9	19.0	−418.01929	19.9	19.0
8	C_{2v}	2	2	−417.21171	13.2	26.0	25.4	−418.01076	25.3	24.6
9	C_{2v}	3	1	−417.18631	12.8	41.9	41.0	−417.98504	41.1	40.4
10	C_s	2	3	−417.18003	13.1	45.9	45.2	−417.98591	40.8	40.1
1 → **2**	C_1	3	3/2	−417.22036	14.0	20.6	20.8	−418.02509	16.6	16.8
2 → **3**	C_s	3	2/1	−417.23551	13.2	11.1	10.5	−418.03679	9.2	8.6
3 → **4**	C_s	3	1/0	−417.23528	12.8	11.1	9.2	−418.03409	10.9	8.9
2 → **5**	C_1	3/2	2/3	−417.19685	13.5	35.3	35.6	−418.00483	29.3	29.6
5 → **6**	C_1	2	3/2	−417.23052	13.8	14.2	14.2	−418.03253	11.6	11.6
(1)		2	0	−417.11372	11.4	87.5	85.1	−417.90783	89.8	87.4
(2)		2	0	−417.14023	11.5	70.9	68.6	−417.93224	74.5	72.2
				$OBe_3H_3^+$ cation[d]						
1	C_{3v}	3	3	−120.34197	23.4	35.7	39.9	−120.65505	21.6	25.8
4	D_{3h}	3	0	−120.39884	19.2	0	0	−120.68946	0	0
5	C_s	2	3	−120.33342	23.1	41.1	44.0	−120.64549	27.6	30.5
6	C_{2v}	2	2	−120.35037	21.8	30.4	33.0	−120.65393	22.3	24.9
7	C_{2v}	2	2	−120.34467	20.4	34.0	35.2	−120.64249	29.5	30.7
8	C_{2v}	2	2	−120.31690	21.8	51.4	53.6	−120.61935	44.0	46.2
1 → **4**	C_1	3	3/2	−120.33336	21.7	41.1	43.6	−120.63944	31.4	33.9
5 → **6**	C_1	2	3/2	−120.33344	22.3	41.0	44.1	−120.64083	30.5	33.6
(1)		2	0	−120.26930	17.2	81.3	79.3	−120.55924	81.7	79.7
(2)		2	0	−120.28147	17.7	73.7	72.2	−120.56689	76.9	75.4

[a] The $E_{rel,1}$ and $E_{rel,2}$ values were calculated without and with inclusion of *ZPE* corrections, respectively.
[b] For the sum of decomposition products of $OBe_3X_3^+$ cations through channels (1) and (2).
[c] Our calculations of isomers **1**—**6** of the $OBe_3F_3^+$ ion in the MP2(full) approximation, in which both valence and core electrons are involved in the active space, give close $E_{rel,2}$ values: −0.1, 5.4, 5.3, 3.0, 7.6, and 0 kcal mol^{-1}, respectively.
[d] Structures **2** and **3** of the $OBe_3H_3^+$ cation are barrierlessly transformed into structure **4** upon geometry optimization. Structure **10** undergoes an analogous barrierless transformation into structure **7**. Structure **9** is characterized by one imaginary frequency (66*i*), E_{tot} values of 120.30096 au (HF) and 120.60168 au (MP2), a *ZPE* value of 20.8 kcal mol^{-1}, and $E_{rel,2}$ values of 63.0 kcal mol^{-1} (HF) and 56.7 kcal mol^{-1} (MP2).

5, **7**, and **8** compared to structure **4** (X = H) are ~30 kcal mol^{-1} and larger. All isomers are stable to decomposition: the dissociation limit calculated for isomer **4** of the $OBe_3H_3^+$ cation is equal to 80 and 75 kcal mol^{-1} for channels (1) and (2), respectively.

If the energies are calculated relative to that of structure **1**, the order in which the forms **5**—**8** of the $OBe_3H_3^+$ and $OBe_3F_3^+$ cations are arranged on the energy scale is the same and the relative energies (except for that of structure **7**) are close to each other. The major distinction is observed for the bridgeless isomer **4**, which is obviously preferable in the case of the hydride ion and is ~3 kcal mol^{-1} less stable than the structure **1** in the case of fluoride ion.

From the data in Table 3 it follows that the O—Be bond lengths in $OBe_3X_3^+$ cations, as well as in the OBe_2X_2, OBe_3X_4, OBe_4X_6, and OBe_2X^+ systems we studied previously,[7—10] are little (to 0.005 Å) dependent on the substituent X. Only for the structure **1** do the O—Be bond lengths in the $OBe_3H_3^+$ and $OBe_3F_3^+$ cations differ by ~0.02 Å. The difference in the bond angles lies in the range from 0 to 10° and that in the torsion angles does not exceed 1° (see Table 4). The *R*(O—Be) distances in asymmetric OBe_k (k = 2, 3)

Table 2. Frequencies (ν_i) and relative intensities (I) of normal vibrations in the IR spectra of isomers **1**—**6** of $OBe_3X_3^+$ (X = H, F) cations

Symmetry	ν_i/cm^{-1} (I (%))	Symmetry	ν_i/cm^{-1} (I (%))	Symmetry	ν_i/cm^{-1} (I (%))	Symmetry	ν_i/cm^{-1} (I (%))	Symmetry	ν_i/cm^{-1} (I (%))
1, X = F		**1, X = H**		**2, X = F**		**3, X = F**		**4, X = F**	
e	299 (1)	e	628 (1)	a″	69 (1)	a′	65 (4)	e′	60 (4)
	299 (1)		628 (1)	a″	188 (2)	a″	89 (4)		60 (4)
a_1	310 (3)	a_1	734 (9)	a′	198 (2)	a″	179 (0)	a_2″	83 (13)
e	558 (18)	e	814 (1)	a′	354 (6)	a′	199 (7)	a_2′	158 (0)
	558 (18)		814 (1)	a″	375 (0)	a″	321 (4)	e″	220 (0)
e	597 (0)	a_2	872 (0)	a′	376 (3)	a′	354 (3)		220 (0)
	597 (0)	e	902 (27)	a′	475 (5)	a′	430 (2)	a_1′	428 (0)
a_2	597 (0)		902 (27)	a″	577 (39)	a′	479 (22)	e′	435 (17)
a_1	763 (5)	a_1	1042 (23)	a′	592 (2)	a′	525 (17)		435 (17)
e	867 (54)	a_1	1114 (21)	a′	694 (14)	a″	530 (70)	a_2″	486 (56)
	867 (54)	e	1316(100)	a′	798 (9)	a′	762 (24)	e′	796 (15)
a_1	902 (57)		1316(100)	a′	935 (87)	a′	1063 (51)		796 (15)
e	995(100)	e	1741 (28)	a′	1227 (18)	a′	1252 (73)	e′	1558(100)
	995(100)		1741 (28)	a′	1318(100)	a′	1454 (53)		1558(100)
a_1	1102 (68)	a_1	1781 (23)	a′	1455 (61)	a′	1601(100)	a_1′	1611 (0)
4, X = H		**5, X = F**		**5, X = H**		**6, X = F**		**6, X = H**	
e′	202 (9)	a″	234 (2)	a″	341 (24)	b_1	57 (1)	b_1	168 (18)
	202 (9)	a″	302 (1)	a′	360 (23)	b_2	226 (2)	a_1	347 (7)
a_2″	211 (8)	a′	330 (15)	a″	484 (1)	a_1	273 (2)	b_1	417 (0)
a_2′	350 (0)	a′	370 (9)	a′	545 (5)	a_2	387 (0)	b_2	425 (3)
e″	449 (0)	a″	371 (0)	a′	813 (15)	b_2	341 (16)	a_1	558 (5)
	449 (0)	a″	447 (38)	a″	899 (0)	b_1	359 (1)	b_2	559 (26)
e′	567 (31)	a′	512 (4)	a″	915 (38)	b_1	484 (70)	a_2	629 (0)
	567 (31)	a′	603 (40)	a′	1044 (8)	a_1	485 (1)	b_1	786 (46)
a_2″	598(100)	a′	691 (33)	a′	1200 (48)	a_1	564 (6)	b_2	1084 (32)
a_1′	792 (0)	a′	718 (45)	a′	1274 (5)	b_2	690 (37)	a_1	1208 (19)
e′	997 (61)	a′	832 (11)	a′	1357 (76)	a_1	855 (35)	a_1	1279 (1)
	997 (61)	a″	973 (78)	a′	1448(100)	b_2	868 (11)	b_2	1384 (100)
e′	2355 (18)	a′	995 (17)	a′	1726 (86)	a_1	1358 (100)	b_2	2002 (4)
	2355 (18)	a′	1199 (91)	a″	1842 (46)	b_2	1410 (84)	a_1	2050 (92)
a_1′	2367 (0)	a′	1395(100)	a′	1935 (27)	a_1	1428 (36)	a_1	2323 (13)

clusters can be varied over a rather wide range, from 1.42 to 1.66 Å at $CN(O) = 3$ and from 1.36 to 1.45 Å at $CN(O) = 2$. Curiously, the averaged R(O—Be) distances for each structure lie, as a rule, in narrow intervals (1.52 to 1.54 Å at $CN(O) = 3$ and 1.40 to 1.42 Å at $CN(O) = 2$) and virtually coincide with R(O—Be) distances in symmetric structures **1**, **4** and **6**, respectively.* This is consistent with calculations of the total overlap populations, ΣQ(O—Be(i)), of all O—Be bonds in OBe_k clusters using the data in Table 5. The corresponding values are nearly constant (they vary over a narrow interval from 1.8 to 2.0) and virtually independent of the CN of the O atom, and are distributed either over three or over two O—Be bonds.

An analogous regularity is observed for the Be—X_b—Be′ bridging bonds (see Table 3). The R(Be—X_b) and R(X_b—Be′) distances also can vary over a wide range (from 1.41 to 1.76 Å for X = F and from 1.36 to 1.69 Å for X = H), whereas the averaged R(X_b—Be) distances, 1.55—1.58 Å (X = F) and 1.48—1.51 Å (X = H), are close to corresponding R(Be—X_b) distances in symmetric Be_2X_4 molecules (1.56 Å for X = F and 1.48 Å for X = H) and OBe_2X^+ cations (1.56 and 1.51 Å for X = F and X = H, respectively) (Fig. 3). The total overlap population (ΣQ(X—Be(i)) ≈ 0.8—0.9) either corresponds to one Be—X_t bond (at $CN(X) = 1$) or is distributed over two bridging bonds, Be—X_b and X_b—Be′ (at $CN(X) = 2$).

In both planar and nonplanar four-membered OBe_2X and XBe_2X cycles the distances between Be atoms (1.9 to 2.2 Å) are close to those in neutral Be_2X_4 molecules and 0.1—0.2 Å longer than in OBe_2X^+ ions (see Fig. 3). In the structures containing n (n = 1, 2, 3) four-membered cycles there are n short (no longer than 2.2 Å) and 3 − n long (>2.8 Å) Be...Be distances; corresponding O...X or X...X distances are close to or somewhat longer than those in OBe_2X^+ ions or in Be_2X_4

* The same values of R(O–Be) distances were obtained for neutral $OBe \cdot nBeX_2$ (X = H, F; n = 1, 2, 3) molecules[7–9] and OBe_2X^+ (X = H, F, Cl) ions.[10]

Table 3. Interatomic distances (R) in isomers **1**—**10** of $OBe_3X_3^+$ (X = H, F) cations

Isomer	Distance	R/Å	
		X = F	X = H
1	O—Be(1)	1.541	1.521
	Be(1)...Be(2)	2.032	1.967
	Be(1)—X_b	1.562	1.513
2	O—Be(1)	1.587	
	O—Be(2)	1.424	
	O—Be(3)	1.581	
	Be(1)...Be(3)	2.156	
	Be(2)...Be(3)	2.009	
	Be(2)—X_b	1.509	
	Be(3)—X_b	1.601	
	Be(1)—X_b·	1.716	
	Be(3)—X_b·	1.448	
	Be(1)—X_t	1.360	
3	O—Be(1)	1.491	
	O—Be(2)	1.455	
	O—Be(3)	1.655	
	Be(2)...Be(3)	2.074	
	Be(2)—X_b	1.443	
	Be(3)—X_b	1.674	
	Be(1)—X_t	1.347	
	Be(3)—X_t·	1.356	
4	O—Be(1)	1.523	1.520
	Be(1)...Be(2)	2.639	2.632
	Be(1)—X_t	1.341	1.310
5	O—Be(1)	1.446	1.441
	O—Be(2)	1.392	1.392
	O...Be(3)	2.752	2.627
	Be(1)...Be(2)	2.308	2.259
	Be(1)...Be(3)	2.050	1.920
	Be(2)...Be(3)	2.437	2.280
	Be(1)—X_b·	1.648	1.595
	Be(2)—X_b	1.533	1.451
	Be(3)—X_b·	1.502	1.413
	Be(3)—X_b	1.560	1.525
6	O—Be(1)	1.407	1.401
	O...Be(3)	3.254	3.039
	Be(1)—X_b	1.476	1.388
	Be(3)—X_b	1.604	1.571
	Be(3)—X_t	1.358	1.315
	Be(1)...Be(2)	2.311	2.275
	Be(1)...Be(3)	2.711	2.495
7	O—Be(1)	1.433	1.433
	O—Be(2)	1.371	1.367
	Be(2)...Be(3)	2.170	2.022
	Be(2)—X_b	1.710	1.696
	Be(3)—X_b	1.430	1.361
	Be(1)—X_t	1.363	1.323
8	O—Be(1)	1.331	1.330
	O—Be(2)	1.476	1.483
	Be(2)...Be(3)	2.176	2.003
	Be(2)—X_b	1.520	1.445
	Be(3)—X_b	1.583	1.517
	Be(3)—X_t	1.364	1.322
9	O—Be(1)	1.361	
	O—Be(2)	1.662	
	Be(2)—X_b	1.544	
	Be(2)...Be(3)	2.221	
	Be(2)—X_t	1.360	
10	O—Be(1)	1.404	
	O—Be(2)	1.457	
	Be(1)...Be(2)	1.933	
	Be(2)...Be(3)	2.184	
	Be(1)—X_b	1.492	
	Be(2)—X_b	1.717	
	Be(2)—X_b·	1.762	
	Be(3)—X_b·	1.419	

molecules. In most structures of $OBe_3X_3^+$ ions the R(Be...Be) distances are considerably (by 0.1—0.2 Å) shorter than the R(O...X) or R(X...X) distances, which is due to larger ionic radii of negatively charged O and X atoms compared to those of Be cations.[10] Correspondingly, the sum of the angles with vertices at the O and X atoms in such cycles is less than 90° (see Table 4), and the four-membered cycles are strained structural elements. The six-membered cycles, in which the angles deviate from 120° (sp^2-hybridization) by no more than ±15°, are much less strained, and the distances between the Be atoms therein are 0.3—0.5 Å longer than in the four-membered cycles. The longest distances between all three Be atoms correspond to the bridgeless structure **4**.

As follows from the data in Table 5, the negative effective charges on oxygen atoms, as well as the O—Be bond lengths, are little dependent on the X substituent and lie in the range from −0.41 to −0.50 au at CN(O) = 3 and from −0.30 to −0.40 au at CN(O) = 2. The negative effective charges of H atoms lie in the range from 0 to −0.20 au and those on F atoms lie in the range from −0.30 to −0.40 au; as usual,[8] bridging X_b atoms bear larger charges than terminal X_t atoms. The charges on Be atoms vary in the range from 0.30 to 0.70 au for X = H and from 0.60 to 1.10 au for X = F. Since in all structures of $OBe_3X_3^+$ cations the distance between Be atoms is shorter than that between O and X atoms and the positive charges on the former (Z(Be)) are always larger, it is the interactions between Be atoms that should make the maxumum contribution to the electrostatic repulsion energy (E_{es}) in each structure. It is obvious that the E_{es} values for the fluoride cation are higher than for the hydride one. For both cations the E_{es} value

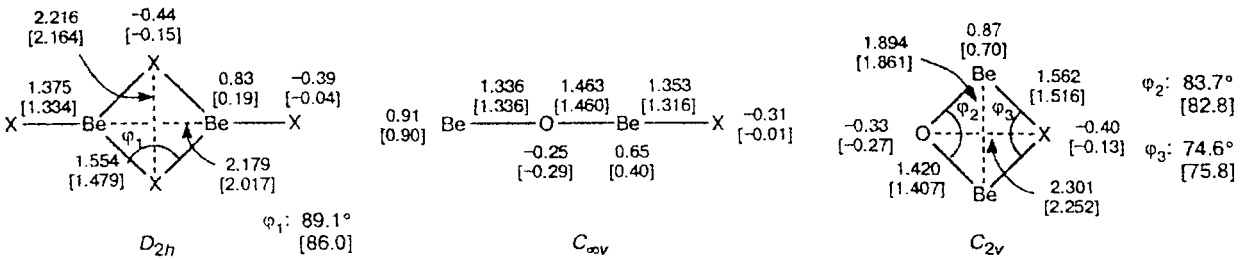

Fig. 3. Structural parameters (bond lengths (R/Å) and bond angles (φ/deg)) and effective charges on the atoms (Z/au) of Be_2X_4 molecules and OBe_2X^+ cations for linear and cyclic structures with X = F and X = H (figures in brackets).

Table 4. Bond (φ) and torsion (θ) angles in isomers **1**—**10** of $OBe_3X_3^+$ (X = H, F) cations

Isomer	Angle	φ, θ/deg	
		X = F	X = H
1	Be(1)—O—Be(2)	82.5	80.4
	Be(1)—X_b—Be(2)	81.1	81.1
	O—Be(1)...Be(2)—X_b	158.2	158.2
2	Be(1)—O—Be(3)	85.8	
	Be(2)—O—Be(3)	83.8	
	Be(1)—X_b·—Be(3)	85.4	
	Be(2)—X_b—Be(3)	80.4	
	O—Be(1)—X_t	142.6	
3	Be(2)—O—Be(3)	83.4	
	Be(1)—O—Be(2)	149.9	
	Be(2)—X_b—Be(3)	83.1	
	O—Be(3)—X_t·	135.3	
	O—Be(1)—X_t	173.7	
5	Be(1)—O—Be(2)	108.9	105.8
	X_b·—Be(3) —X_b·	94.9	99.2
	X_b·—Be(1)—X_b·	84.4	84.8
	O—Be(2)—X_b	125.8	129.1
	Be(2)—X_b—Be(3)	104.0	100.0
	X_b·—Be(3)...Be(1)...Be(2)	112.0	111.0
6	Be(1)—O—Be(2)	110.5	108.5
	X_b—Be(3)—X_b	104.7	114.9
	O—Be(1)—X_b	123.2	133.4
7	X_b—Be(2)—X_b	82.3	83.6
	X_b—Be(3)—X_b	103.8	112.4
8	X_b—Be(2)—X_b	93.3	98.0
	X_b—Be(3)—X_b	88.6	91.9
9	Be(2)—O—Be(3)	83.8	
	Be(1)—X_b·—Be(3)	92.1	
	O—Be(2)—X_t	124.8	
10	Be(1)—O—Be(2)	85.0	
	Be(2)—X_b—Be(3)	73.7	
	X_b·—Be(2)—X_b·	80.8	
	X_b·—Be(3)—X_b·	107.2	
	Be(1)—Be(2)—Be(3)	166.4	
	O—Be(1)—X_b	107.2	
	Be(2)—X_b·...X_b·—Be(3)	177.7	
	X_b·—Be(2)...Be(3)—X_b·	177.9	

increases as the number of bridging X_b atoms and that of four-membered cycles with short Be...Be distances increases. For this reason, the destabilizing effect due to electrostatic repulsion is maximum in structure **1** with three bridging X atoms and three four-membered cycles and is minimum in structure **4**; for the planar form **6** this effect is somewhat more pronounced than for **4**.

Another destabilizing factor is a strain in four-membered cycles. From this point of view, the structure **1** with three and structures **2** and **10** with two such cycles are the most unstable. Since the lengths of bridging Be—H—Be and Be—F—Be bonds and the angles in the cycles are close, one can suggest that the effect of this factor on the $OBe_3H_3^+$ and $OBe_3F_3^+$ cations is nearly the same. Finally, the third destabilizing factor can be the presence of terminal Be atoms with unsaturated valences and *CN* = 1 (structures **8** and **9**).

Among stabilizing factors the most important are the following: the number of strong O—Be bonds (particularly in the structures **1**—**4** and **9**), the number of strong bridging Be—X—Be bonds, and the possibility of the formation of additional O→Be and F→Be donor-acceptor π-bonds stabilizing the planar forms **2**—**4** and **6**—**9** and the planar fragment in structure **5**.

Judging from the dimerization energies of BeX_2 molecules, the fluoride Be—F_b—Be bridges are ~8—10 kcal mol^{-1} more stable than the hydride Be—H_b—Be bridges.[7—9] At the same time, the electrostatic repulsion between the Be atoms in the fluoride cation is stronger than in the hydride cation due to a higher polarity of the former. These factors compensate each other in structures **5**, **6**, and **8**. The sharp difference in the relative stability of structures **1** and **4** is likely due to the large difference in the strength of the three fluoride and hydride bridges. For the $OBe_3H_3^+$ cation, the bridgeless structure **4** with minimum electrostatic repulsion is the most favorable, whereas in the case of the $OBe_3F_3^+$ cation, the isomers **1** and **4** are close in energy. The high stability of the form **6** and the planar structure of isomer **2** of the $OBe_3F_3^+$ cation is most likely due to the formation of F→Be donor-acceptor π-bonds despite the presence of two strained adjacent four-membered cycles and lengthening of several fluoride bridges in structure **2**.

The wave functions of almost each isomer of $OBe_3X_3^+$ cations with *CN*(O) = 2 can be represented as a superposition of covalent and ionic components. The analysis of structural parameters and effective charges on the atoms of isomers **7** and **10** and comparison with analogous data for OBe_2X^+ cations (see Fig. 3) suggest that the major contribution to their wave functions comes from a structure of the $OBe_2X^+ \cdot BeX_2$ type with the bidentate coordination of the BeX_2 molecule to one of the Be atoms of the linear or cyclic form of the OBe_2X^+ ion. Therefore, a barrierless transformation of structure **10** into **7**, caused by the breaking of a weak Be(2)—H_b bond, is natural for the $OBe_3H_3^+$ hydride, whereas the stronger Be(2)—F_b bond in the $OBe_3F_3^+$ fluoride is not cleaved, despite its weakening and lengthening up to 1.72 Å. The state of isomers **5**, **6**, and **8** can be described by superposition of a covalent structure and the structure of the $OBe_2^{2+} \cdot BeX_3^-$ ion pair with tri- and bidentate coordination of the BeX_3^- anion to both Be atoms (structures **5** and **6**, respectively) and its bidentate coordination to one of the Be atoms (**8**) of the OBe_2^{2+} dication. For isomer **6** one should take into account the

Table 5. Effective charges on atoms (Z(A)) and Mulliken overlap populations of bonds (Q(A—B)) for isomers of $OBe_3X_3^+$ (X = H, F) cations

Isomer	Atom, bond	Z/au, [Q]/au X = F	X = H
1	O	−0.50	−0.41
	Be	0.91	0.66
	X_b	−0.41	−0.19
	O—Be	[0.60]	[0.55]
	Be—X_b	[0.39]	[0.39]
2	O	−0.45	
	Be(1)	0.77	
	Be(2)	0.89	
	Be(3)	0.89	
	X_b	−0.38	
	X_b·	−0.37	
	X_t	−0.34	
	O—Be(1)	[0.53]	
	O—Be(2)	[0.88]	
	O—Be(3)	[0.40]	
	Be(1)—X_b·	[0.24]	
	Be(3)—X_b·	[0.59]	
	Be(2)—X_b	[0.44]	
	Be(3)—X_b	[0.37]	
	Be(1)—X_t	[0.84]	
3	O	−0.46	
	Be(1)	0.70	
	Be(2)	0.92	
	Be(3)	0.80	
	X_b	−0.37	
	X_t	−0.29	
	X_t·	−0.33	
	O—Be(1)	[0.79]	
	O—Be(2)	[0.77]	
	O—Be(3)	[0.37]	
	Be(1)—X_t	[0.86]	
	Be(2)—X_b	[0.55]	
	Be(3)—X_b	[0.27]	
	Be(3)—X_t·	[0.85]	
4	O	−0.41	−0.50
	Be	0.73	0.50
	X_t	−0.26	0
	O—Be	[0.68]	[0.65]
	Be—X_t	[0.88]	[0.84]
5	O	−0.40	−0.36
	Be(1)	0.84	0.68
	Be(2)	0.78	0.59
	Be(3)	1.03	0.51
	X_b·	−0.41	−0.13
	X_b	−0.42	−0.16
	O—Be(1)	[0.83]	[0.83]
	O—Be(2)	[0.98]	[0.98]
	Be(1)—X_b·	[0.31]	[0.27]
	Be(2)—X_b	[0.42]	[0.46]
	Be(3)—X_b·	[0.39]	[0.39]
	Be(3)—X_b	[0.48]	[0.55]
6	O	−0.36	−0.32
	Be(1)	0.82	0.62
	Be(3)	0.88	0.40
	X_b	−0.41	−0.15
	X_t	−0.34	−0.03
	O—Be(1)	[0.92]	[0.92]
	Be(1)—X_b	[0.50]	[0.55]
	Be(3)—X_b	[0.33]	[0.32]
	Be(3)—X_t	[0.84]	[0.86]
7	O	−0.33	−0.34
	Be(1)	0.57	0.33
	Be(2)	0.74	0.56
	Be(3)	1.09	0.60
	X_b	−0.37	−0.06
	X_t	−0.33	−0.02
	O—Be(1)	[0.91]	[0.89]
	O—Be(2)	[1.05]	[1.08]
	Be(1)—X_t	[0.83]	[0.85]
	Be(2)—X_b	[0.23]	[0.18]
	Be(3)—X_b	[0.59]	[0.65]
8	O	−0.31	−0.29
	Be(1)	0.88	0.86
	Be(2)	0.82	0.43
	Be(3)	0.84	0.26
	X_b	−0.43	−0.14
	X_t	−0.35	0
	O—Be(1)	[1.18]	[1.19]
	O—Be(2)	[0.75]	[0.76]
	Be(2)—X_b	[0.42]	[0.43]
	Be(3)—X_b	[0.36]	[0.39]
	Be(3)—X_t	[0.83]	0.81]
9	O	−0.48	
	Be(1)	1.02	
	Be(2)	0.80	
	X_b	−0.40	
	X_t	−0.37	
	O—Be(1)	[1.05]	
	O—Be(2)	[0.35]	
	Be(2)—X_b	[0.41]	
	Be(1)—X_t	[0.83]	
10	O	−0.43	
	Be(1)	0.72	
	Be(2)	0.85	
	Be(3)	1.05	
	X_b	−0.44	
	X_b·	−0.37	
	O—Be(1)	[0.93]	
	O—Be(2)	[0.75]	
	Be(2)—X_b·	[0.21]	
	Be(3)—X_b·	[0.61]	
	Be(1)—X_b	[0.47]	
	Be(2)—X_b	[0.23]	

contribution of the $OBe_2X_2 \cdot BeX^+$ structure since the X_b atoms are 0.13 Å (X = F) and 0.19 Å (X = H) closer to Be atoms bonded to the O atom.

According to MP2 calculations of the $OBe_3F_3^+$ cation (see Tables 1 and 6), the barriers to rearrangements **2** → **3**, **3** → **4**, and **5** → **6** occurring with the breaking of one fluoride bridge lie in the range 2.8—3.7 kcal mol^{-1}. The F_b atom in the transition state is displaced from its equilibrium position in the initial structure (toward the final one) by 0.50 to 0.70 Å, and the earliest transition state (0.50 Å) is found for the rearrangement **5** → **6**. The energy barrier to rearrangement **1** → **2** is appreciably higher (16.2 kcal mol^{-1}) and the shift of the bridging F_b atom from its position in structure **1** (X = F) is about 1 Å.

For comparison, we performed calculations of minimum energy pathways and found the transition states of two rearrangements occurring with the breaking of hydride bridges in the isomers **1** and **5** of the $OBe_3H_3^+$ cation (see Table 1). In contrast to the fluoride analog, the shift of the bridging H_b atom by 0.8 Å from its equilibrium position in structure **1** (X = H) causes simultaneous cleavage of two other Be—H—Be bridging bonds, and this structure is immediately transformed into the most favorable bridgeless form **4** (X = H) with overcoming of a barrier of ~8 kcal mol^{-1}, bypassing corresponding two- and one-bridge forms **2** and **3**, respectively. The energy barrier to rearrangement **5** → **6** for the $OBe_3H_3^+$ cation (~3 kcal mol^{-1}) is also lower than for the $OBe_3F_3^+$ cation.

If the F_t atom in isomer **2** of the $OBe_3F_3^+$ cation approaches the Be(3) atom with CN = 3 without imposing symmetry (C_1) restrictions, the O—Be bond is cleaved simultaneously with the formation of a fluoride bridge (the rearrangement **2** → **5**). In the transition state of this rearrangement the F_t atom is at a distance of 1.42 Å

Table 6. Imaginary frequencies (ν), interatomic distances (R), and bond (φ) and torsion (θ) angles of transition states (TS) of intramolecular rearrangements of $OBe_3F_3^+$ cation

TS (ν/cm^{-1})	Distance	R/Å	Angle	φ, θ /deg
1 → **2**	O—Be(1)	1.600	Be(2)—O—Be(3)	83.9
(189*i*)	O—Be(2)	1.459	Be(1)—O—Be(3)	82.0
	O—Be(3)	1.559	Be(1)—O—Be(2)	101.3
	Be(1)—F_b·	1.636	Be(2)—F_b—Be(3)	80.5
	Be(1)—F_t	1.399	Be(1)—F_b·—Be(3)	83.0
	Be(2)—F_b	1.506	F_t—Be(1)—O	112.9
	Be(3)—F_b	1.616	F_b—Be(2)...Be(3)—O	170.4
	Be(3)—F_b·	1.488	F_b·—Be(1)...Be(3)—O	158.5
	Be(2)—F_t	2.529	F_t—Be(1)...Be(2)—O	152.8
2 → **3**	O—Be(1)	1.518	Be(2)—O—Be(3)	83.5
(178*i*)	O—Be(2)	1.432	Be(1)—O—Be(3)	96.4
	O—Be(3)	1.627	Be(2)—F_b—Be(3)	82.0
	Be(2)—F_b	1.484	F_t·—Be(3)—O	108.4
	Be(3)—F_b	1.623	F_t—Be(1)—O	160.9
	Be(1)—F_t·	2.241	F_b—Be(2)—O	104.3
	Be(1)—F_t	1.352	F_b—Be(3)—O	90.2
	Be(3)—F_t·	1.390	Be(2)—O—Be(3)	83.9
2 → **5**	O—Be(1)	1.539	Be(2)—O—Be(3)	80.6
(288*i*)	O—Be(2)	1.407	Be(1)—O—Be(3)	71.0
	O—Be(3)	1.734	Be(2)—F_b—Be(3)	82.8
	Be(2)—F_b	1.513	Be(1)—F_b·—Be(3)	72.9
	Be(3)—F_b	1.582	F_t—Be(1)—O	108.1
	Be(1)—F_b·	1.721	F_b—Be(2)—O	106.8
	Be(3)—F_b·	1.471	F_b—Be(2)...Be(3)—O	179.8
	Be(1)—F_t	1.431	Be(1)...Be(2)...Be(3)—O	165.9
	Be(3)—F_t	2.083	F_b·—Be(1)...Be(3)—O	127.5
			F_t—Be(1)...Be(3)—O	121.6
3 → **4**	O—Be(1)	1.502	F_t—Be(1)—O	173.7
(159*i*)	O—Be(2)	1.501	F_t·—Be(2)—O	120.2
	O—Be(3)	1.554	F_t·—Be(3)—O	159.7
	Be(1)—F_t	1.344		
	Be(2)—F_t·	1.365		
	Be(3)—F_t·	1.345		
	Be(3)—F_t·	2.377		
5 → **6**	O—Be(1)	1.424	Be(1)—O—Be(2)	110.8
(189*i*)	O—Be(2)	1.400	F_b—Be(3)—O	66.9
	O—Be(3)	2.788	F_b—Be(2)—O	127.3
	Be(2)—F_b	1.511	F_b·—Be(1)—O	123.5
	Be(3)—F_b	1.578	F_t—Be(3)—O	76.7
	Be(1)—F_b·	1.529	Be(1)—F_b·—Be(3)	89.8
	Be(3)—F_b·	1.565	F_b—Be(1)...Be(2)—O	179.5
	Be(3)—F_t	1.416	Be(3)...Be(1)...Be(2)—O	169.2
	Be(1)—F_t	2.148	F_b·—Be(1)...Be(2)—O	153.6
			F_t—Be(1)...Be(3)—F_b·	132.6

(0.58 Å) from its equilibrium position in the structure **2** (**5**), and the O—Be(3) bond is only 0.15 Å longer than in isomer **2**. In this case the energy barrier is ~25 kcal mol^{-1}. Thus, the isomers **1**, **4**, and **6** (X = F) are separated from the other isomers by rather high (from 11 to 25 kcal mol^{-1}) or appreciable (~6 kcal mol^{-1} between isomers **3** and **4**) barriers and are likely to be observed at moderate (**4**) and even elevated (**1** and **6**) temperatures. The remaining forms (**2**, **3**, and **5**) of the $OBe_3F_3^+$ cation can be stabilized only in inert matrices at low temperatures.

Several assumptions can be made of changes in the relative arrangement of key structures **1**, **4**, and **6** of $YM_3X_3^+$ (Y, X, and M are chalcogen, halogen, and alkaline-earth metal atoms, respectively) cations on the energy scale in the case of replacement of light Y, M, and X atoms by their heavier analogs in the subgroups of the Periodic system. For instance, the Be—Cl—Be and Mg—H—Mg bridges are almost as strong as the Be—H—Be bridging bonds; however, the lengthening of the Be—Cl, O—Mg, and Mg—H bonds upon replacement of H by Cl or Be by Mg should result in flattening of the OM_3 pyramid in the structure **1**, lengthening of the distances between metal atoms, and hence, in a reduction of the electrostatic repulsion and approach of the relative energies of forms **1** and **4** as compared to those of the corresponding forms of the $OBe_3H_3^+$ cation. For the same reasons, replacement of the O atom by S atom should lead to stabilization of isomer **1** with X = H compared to corresponding isomer **4**. The latter, with three terminal H atoms in the $SM_3H_3^+$ cation, will likely have C_{3v} symmetry since a pyramidal structure is characteristic of a tricoordinate S atom. For fluoride cations with Y = O, S and M = Be, Mg and most strong fluoride M—F—M bridges the structure **1** should be the most favorable. Appreciable stabilization of the planar form **6** is most probable for beryllium fluorides, since the strength of Y→M and X→M donor-acceptor π-bonds decreases sharply if the Y(X) and M atoms belong either to different periods or to the second row of the Periodic system.

As can be seen from the data in Table 2, all planar structures are characterized by low frequencies of the out-of-plane and in-plane bending vibrations (60—70 and 170—200 cm^{-1} for the $OBe_3F_3^+$ and $OBe_3H_3^+$ cation, respectively), which, taken together with the low energy barriers to intramolecular rearrangements, indicates their structural nonrigidity. The highest frequencies of bending vibrations (300 and 600—700 cm^{-1} for the $OBe_3F_3^+$ and $OBe_3H_3^+$ cations, respectively) were found for the most rigid three-bridge forms of **1** separated from other structures by higher barriers.

Our calculations revealed that the frequencies of stretching vibrations (in the region 800—1600 cm^{-1}) of the key isomers **1**, **4**, and **6** are appreciably different. For instance, four intense bands corresponding to the vibrations of the O—Be and Be—F bonds were found in the IR spectrum of the C_{3v} isomer **1** of the $OBe_3F_3^+$ cation in the region 850—1100 cm^{-1}. There are only two intense bands in the IR spectrum of isomer **4** (X = F) with D_{3h} symmetry; one of them, of the e′ symmetry (at ~1500 cm^{-1}), corresponds to stretching vibrations of Be atom in the linear O—Be—F fragment, while the other band (at ~500 cm^{-1}) corresponds to the a_2'' type out-of-plane bending vibration of the OBe_3 polyhedron. On the contrary, the most intense band (at ~600 cm^{-1}) in the spectrum of isomer **4** of the $OBe_3H_3^+$

cation corresponds to the a_2'' type bending vibration, while the less intense e′ type band (at ~1000 cm^{-1}) corresponds to the stretching vibration of the O—Be bonds (the vibrations of the O—Be and Be—H bonds of this isomer are observed in different spectral regions). Finally, there are six rather intense bands in the region 500—1400 cm^{-1} in the spectrum of the planar isomer **6** (X = F) with C_{2v} symmetry.

A more complex picture is observed for the C_s structures **2**, **3**, and **5** of the $OBe_3F_3^+$ cation, which are characterized by a large number of intense bands in the region 600—1600 cm^{-1}. The most intense band in the IR spectrum of isomer **3** lies near 1600 cm^{-1} (the stretching vibration of the O—Be—F fragment, like in structure **4**), whereas in the spectra of isomers **2** and **5** (and **6**) they lie in the region 1300—1400 cm^{-1}. These distinctions can be used for experimental identification of isomers, *e.g.*, by matrix-isolation IR spectroscopy.

The authors express their gratitude to the Alabama Computational Network and to the N. D. Zelinsky Institute of Organic Chemistry, Russian Academy of Sciences, for providing computational resources on SGI, SUN, and Power Challenger workstations.

This work was partially supported by the Russian Foundation for Basic Research (Project No. 93-03-04486).

References

1. V. A. Sipachev and Yu. S. Nekrasov, *Org. Mass. Spectrom.*, 1988, **23**, 809.
2. K. S. Krasnov, N. V. Filippenko, V. A. Bobkova, N. L. Lebedeva, E. V. Morozov, T. I. Ustinova, and G. A. Romanova, *Molekulyarnye postoyannye neorganicheskikh soedinenii* [*Molecular Constants of Inorganic Compounds*], Ed. K. S. Krasnov, Khimiya, Leningrad, 1979, 448 pp. (in Russian).
3. N. M. Klimenko, V. G. Zakzhevskii, and O. P. Charkin, *Koord. Khim.*, 1982, **10**, 325 [*Sov. J. Coord. Chem.*, 1982, **10** (Engl. Transl.)].
4. A. M. Mebel', N. M. Klimenko, and O. P. Charkin, *Zh. Strukt. Khim.*, 1988, **29**, No. 3, 12 [*J. Struct. Chem. (USSR)*, 1988, **29**, 357 (Engl. Transl.)].
5. N. M. Klimenko, in *Khimicheskaya svyaz' i stroenie molekul* [*The Chemical Bond and Molecular Structure*], Nauka, Moscow, 1984, 36 (in Russian).
6. P. v. R. Schleyer, *New Horizons in Quantum Chemistry*, Dordrecht, Reidel—New York, 1983, 427 pp.
7. E. A. Rykova and N. M. Klimenko, *Zh. Neorg. Khim.*, 1995, **40**, 1879 [*Russ. J. Inorg. Chem.*, 1995, **40**, 1810 (Engl. Transl.)].
8. E. A. Rykova, N. M. Klimenko, and A. I. Grigor'ev, *Int. J. Quant. Chem.*, 1996, **57**, 697.
9. E. A. Rykova and N. M. Klimenko, *Int. Workshop "Small Mol. Indaba," Abstrs.*, South Africa, 1995, 14.
10. N. M. Klimenko and Zh. E. Grabovskaya, *Zh. Neorg. Khim.*, 1999, **44**, No. 3 [*Russ. J. Inorg. Chem.*, 1999, **44**, No. 3 (Engl. Transl.)].
11. M. W. Schmidt, K. K. Baldridge, J. A. Boatz, S. T. Elbert, M. S. Gordon, J. H. Jensen, S. Koseki, N. Matsunaga, K. A. Nguyen, S. J. Su, T. L. Windus, M. Dupuis, and J. A. Montgomery, *J. Comput. Chem.*, 1993, **14**, 1347.
12. M. J. Frisch, G. W. Trucks, H. B. Schlegel, P. M. W. Gill, B. G. Johnson, M. A. Robb, J. R. Cheeseman, T. Keith, G. A. Petersson, J. A. Montgomery, K. Raghavachari, M. A. Al-Laham, V. G. Zakrzewski, J. V. Ortiz, J. B. Foresman, J. Cioslowski, B. B. Stefanov, A. Nanayakkara, M. Challacombe, C. Y. Peng, P. Y. Ayala, W. Chen, M. W. Wong, J. L. Andres, E. S. Replogle, R. Gomperts, R. L. Martin, D. J. Fox, J. S. Binkley, D. J. Defrees, J. Baker, J. P. Stewart, M. Head-Gordon, C. Gonzalez, and J. A. Pople, *GAUSSIAN-94, Revision C.2*, Gaussian Inc., Pittsburgh (PA), 1995.
13. N. M. Klimenko, E. A. Rykova, and M. L. McKee, *XVI Austin Symp. on Mol. Struct., Abstrs.*, Austin (Texas, USA), 1996, 129.
14. E. A. Rykova, M. L. McKee, I. N. Senchenya, and N. M. Klimenko, *Vseros. konf. po teor. khimii, Tez. dokl.* [*Abstrs. All-Russian Conf. on Theor. Chem.*], Kazan' (Russia), 1997, 65 (in Russian).

Received July 20, 1998